# New Pyridinone Derivatives as Potent HIV-1 Nonnucleoside Reverse Transcriptase Inhibitors

Kiet Le Van,[†,§] Christine Cauvin,[*,‡,§] Stéphane de Walque,[‖,§] Benoît Georges,[†] Sandro Boland,[‡] Valérie Martinelli,[‖]
Dominique Demonté,[‖] François Durant,[‡,#] László Hevesi,[†,#] and Carine Van Lint[‖,#]

*Laboratoire de Chimie des Matériaux Organiques and Laboratoire de Chimie Moléculaire Structurale, Facultés Universitaires Notre-Dame de la Paix (FUNDP), B-5000 Namur, Belgium, and Laboratoire de Virologie Moléculaire, Institut de Biologie et de Médecine Moléculaires, Université Libre de Bruxelles (ULB), B-6041 Gosselies, Belgium*
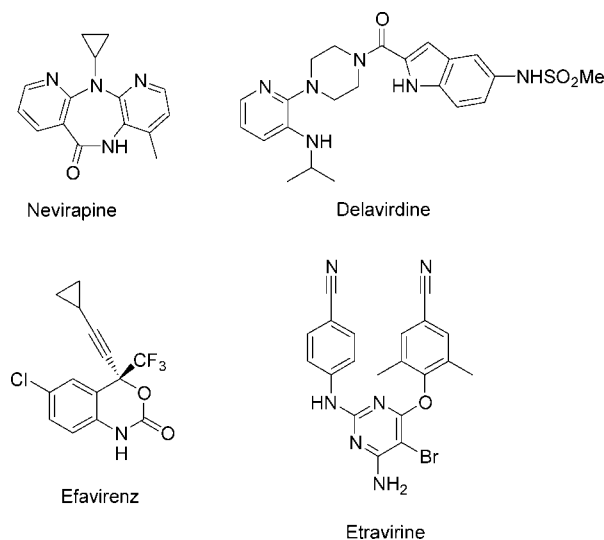
Several 5-ethyl-6-methyl-4-cycloalkyloxy-pyridin-2(1*H*)-ones were synthesized and evaluated for their anti HIV-1 activities against wild-type virus and clinically relevant mutant strains. A racemic mixture (**10**) with methyl substituents at positions 3 and 5 of the cyclohexyloxy moiety had potent antiviral activity against wild-type HIV-1. Subsequent stereoselective synthesis of a stereoisomer displaying both methyl groups in equatorial position was found to have the best EC$_{50}$. Further modulations focused on position 3 of the pyridinone ring improved the antiviral activity against mutant viral strains. Compounds bearing a 3-ethyl (**22**) or 3-isopropyl group (**23**) had the highest activity against wild-type HIV-1 and displayed low-nanomolar potency against several clinically relevant mutant strains.
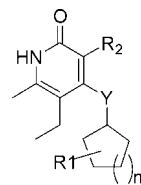
## Introduction

Reverse transcriptase (RT[a]) is a key enzyme of the human immunodeficiency virus type 1 (HIV-1) life cycle. It is responsible for the transformation of HIV genomic single-stranded RNA into double-stranded proviral DNA. RT has been recognized as an attractive target for drug development for a number of years, and numerous RT inhibitors have been developed.[1] Nucleoside reverse transcriptase inhibitors (NRTIs), such as azidothymidine (AZT), are activated in cells and then act as decoy substrates and chain terminators, thereby preventing the synthesis of a functional double-stranded DNA. Nonnucleoside reverse transcriptase inhibitors (NNRTIs) are a structurally diverse class of compounds that inhibit the enzyme by binding to a specific allosteric pocket located some 10 Å from the polymerase active site.[2,3] To date, four NNRTIs (nevirapine, delavirdine, efavirenz, and etravirine) have been approved for clinical use (Figure 1).[4] Combination of NRTIs and NNRTIs with other antiviral agents, such as viral protease inhibitors (e.g., saquinavir, indinavir, amprenavir, lopinavir, darunavir,...) or fusion inhibitors (enfuvirtide) or integrase inhibitors (raltegravir), led to the development of highly active antiretroviral therapy (HAART) that allows an important decrease in viral load and a significant improvement of the patient's health.[5] In spite of these major advances, new and potent anti-HIV compounds are still needed because of the continued emergence of mutant viral strains that are resistant to current antiretroviral agents.[6]

Pyridinone derivatives were first described as NNRTIs in 1991.[7] More recently, several NNRTIs based on the pyridinone

* To whom correspondence should be addressed. Phone: +32 81 72 45 69. Fax: +32 81 72 54 40. E-mail: christine.cauvin@fundp.ac.be.
† Laboratoire de Chimie des Matériaux Organiques, Facultés Universitaires Notre-Dame de la Paix.
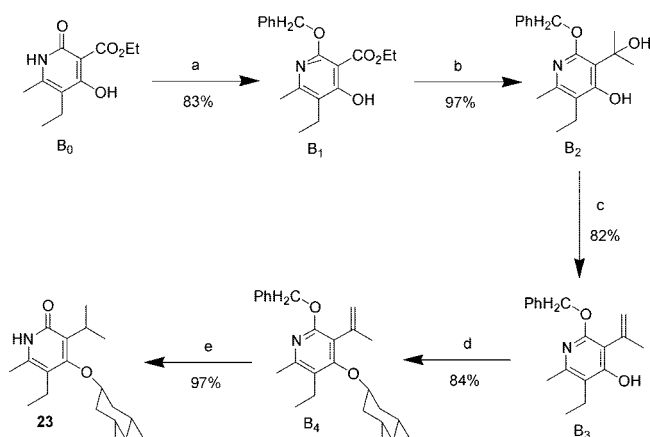§ These authors contributed equally to this work.
‡ Laboratoire de Chimie Moléculaire Structurale, Facultés Universitaires Notre-Dame de la Paix.
‖ Université Libre de Bruxelles.
# These authors codirected the present study. C.V.L. is Directeur de Recherches of the Belgian "Fonds de la Recherche Scientifique-FNRS" (FRS-FNRS).
a Abbreviations: RT, reverse transcriptase; HIV-1, human immunodeficiency virus type 1; NNRTI, nonnucleoside reverse transcriptase inhibitor; EC$_{50}$, 50% effective concentration; CC$_{50}$, 50% cytotoxic concentration; SI, selectivity index.

**Figure 1.** Chemical structures of commercial NNRTIs.



**Figure 2.** General structure of 4-cycloalkyloxypyridin-2(1*H*)-one derivatives.

scaffold have been reported such as 4-arylthiopyridin-2(1*H*)-one compounds.[8] Despite several studies pointing out compound flexibility as an important parameter for conserving potency on various mutant viral strains, the pyridinone compounds previously described only include arylthio, aryloxy, or benzyl moieties at position 4 of the pyridinone ring.[9,10] We now report in this study the design, synthesis, and HIV-1 inhibiting properties of a new series of potent 4-cycloalkyloxypyridin-2(1*H*)-one derivatives (Figure 2). Optimization of this series led to the identification of compounds combining high potency

**Scheme 1.** Synthesis of Derivative **23**[a]



[a] Reagents and reaction conditions: (a) PhCH$_2$Br, Ag$_2$CO$_3$, PhH, 60 °C, 20 h; (b) MeLi (3.5 equiv), THF, −78 °C (1 h), then 0 °C (3 h); (c) SOCl$_2$, PhH, 5 °C to room temp, 2 h; (d) 3,5-dimethylcyclohexanol (α isomer), DIAD, PPh$_3$, THF, room temp, 20 h; (e) H$_2$, 1 atm, Pd/C, EtOH, room temp, 36 h.

**Scheme 2.** Synthesis of Derivative **22**[a]
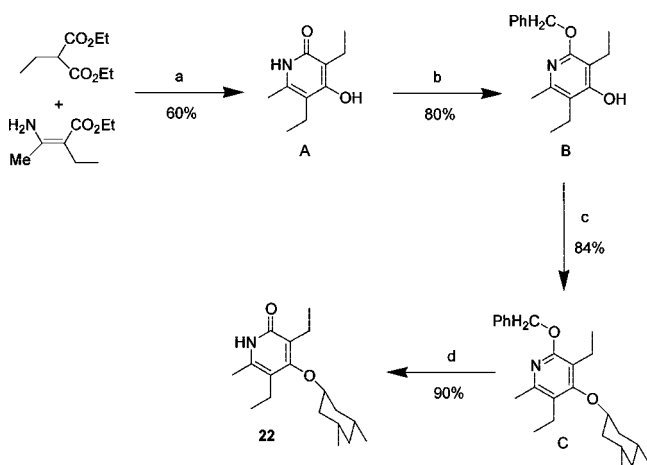


[a] Reagents and reaction conditions: (a) NaOEt, EtOH, toluene, reflux, 60 h; (b) PhCH$_2$Br, Ag$_2$CO$_3$, C$_6$H$_6$, 80 °C, 6 h; (c) 3,5-dimethylcyclohexanol (α isomer), DIAD, PPh$_3$, THF, room temp, 24 h; (d) cyclohexene, Pd/C, *i*-Pr$_2$O, 80 °C, 6 h.
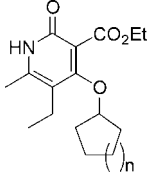
against wild-type HIV-1 and a panel of single and double mutant strains with very low cytotoxicity.

## Chemistry

Almost all the compounds studied have been synthesized from the common intermediate **B$_0$**, which is easily obtained from ethyl 2-acetylbutyrate, ammonia, and diethyl malonate. Scheme 1 shows a typical example in the case of compound **23**. The synthetic route began by the O-benzylation of **B$_0$** to give **B$_1$**. This compound was subjected to reductive methylation yielding **B$_2$**. Dehydration was performed with thionylchloride to afford **B$_3$**. Then Mitsunobu reaction with 3,5-dimethylcyclohexanol gave **B$_4$**. This last compound led to **23** after extensive catalytic hydrogenation.

A slight modification of the general synthetic pathway is illustrated for compound **22** (Scheme 2). Intermediate **A** was obtained by condensation of ethyl 3-amino-2-ethylbutenoate with diethyl 2-ethylmalonate. O-Benzylation of **A** gave **B**, which underwent Mitsunobu reaction with 3,5-dimethylcyclohexanol

**Table 1.** In Vitro RT Assays, Antiviral Activity against Wild-Type HIV-1 Virus, and Selectivity Index of Pyridinone Compounds with Various Alkyl Rings



| compd | n | % RT residual activity[a] | EC$_{50}$ (μM)[b] | SI[c] |
|-------|---|---------------------------|-------------------|-------|
| **1** | 1 | 58.6 | 0.74 | >135 |
| **2** | 2 | 44.7 | 0.23 | >435 |
| **3** | 3 | 34.6 | 0.39 | 205 |
| **4** | 4 | 24.0 | 0.70 | 83 |

[a] Percentage of RT residual activity after addition of 10 μM compound. [b] Effective concentration 50%. [c] Selectivity index or ratio of CC$_{50}$ to EC$_{50}$.

yielding **C**. Finally, debenzylation by catalytic hydrogenation led to **22** in high yield.

## Results and Discussion

In the first step, impact of the cycloalkyl ring size was evaluated. Compounds **1**−**4** containing rings ranging from cyclopentyl to cyclooctyl were prepared from **B$_0$** (Table 1). These four pyridinone derivatives effectively inhibited RT at 10 μM in an in vitro enzymatic assay. All compounds subsequently displayed moderate antiviral activity with EC$_{50}$ values ranging from 0.2 to 0.7 μM.

Molecular modeling of compounds into the allosteric site was performed using a RT structure extracted from RT-TNK-651 complex (PDB code 1RT2[11]). Molecular docking algorithms implemented in Gold[12] were used in order to provide binding mode hypotheses, which were then refined using Accelrys Discover 3 module.[13,14] Figure 3 displays a schematic drawing of the best-ranking binding mode of **2**. It is consistent with binding modes experimentally observed for similar derivatives.[15] The pyridinone ring is pinned between Leu100 and Val106, allowing the lactam NH to form a hydrogen bond with Lys101. The hydrophobic 5-Et group faces Tyr181, favoring the conformational change required for efficient inhibition.[11] The 4-cycloalkoxy group of the inhibitor is located in the most hydrophobic part of the binding pocket, interacting with Tyr181, Tyr188, Phe227, and Trp229. Finally, the ester moiety of the compound is located near Pro236, in the most flexible part of the NNRTI binding pocket. From modeling results and structure−activity relationships, it can be pointed out that the cyclohexyl ring (**2**) was the best compromise between occupation of the hydrophobic pocket and conformational energy penalties.

Replacement of the hydrophobic cyclohexyl ring by a more hydrophilic piperidine ring resulted in a dramatic loss of activity, consistent with SAR from other NRRTI series, where hydrophobic substituents are also favored in this position.

In the second step, the effect of substitution on this cyclohexyl ring was investigated either in the P4 cell line or in the TZM-bl cell line (compounds **5**−**10** in Table 2). These compounds were synthesized as mixtures of stereoisomers. From comparison of the antiviral activity of these compounds, it can be observed that "meta" (i.e., 3,5) substitution was favored over "ortho" and "para" substitutions. Compound **10** with methyl substituents in positions 3 and 5 had an antiviral potency (0.043 μM), similar to nevirapine (0.039 μM, Table 2). This mixture of isomers was separated by chiral HPLC, giving two main fractions **10A**
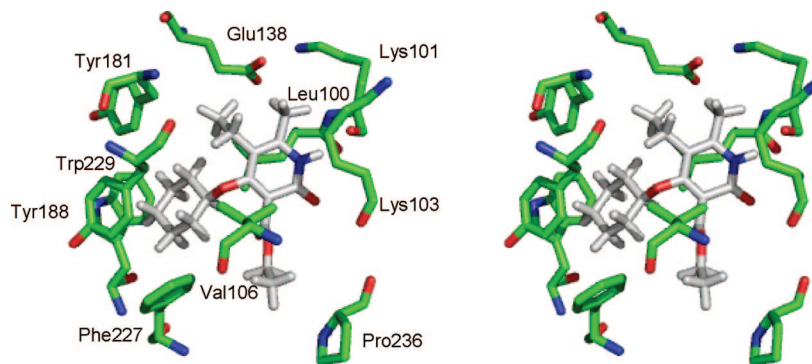
**Figure 3.** Stereoscopic view of the binding mode of **2** (only main surrounding residues are shown in green).

**Table 2.** Antiviral Activity against Wild-Type HIV-1 Virus in TZM-bl Cells and Selectivity Index of Compounds with Substituent Variations at Positions 3 and 4 of the Pyridinone Ring: Comparison with the Reference Compounds Nevirapine and Efavirenz



| compd | $R_1$ | Y | $R_2$ | $EC_{50}$ ($\mu$M) | SI |
|---|---|---|---|---|---|
| **5** | 2-Cl[a] | O | $CO_2Et$ | >3.0[c] | <33 |
| **6** | 3-$CH_3$[a] | O | $CO_2Et$ | 0.520[c] | 192 |
| **7** | 4-$CH_2CH_3$[a] | O | $CO_2Et$ | >4.0[c] | <14 |
| **8** | 2,3-di$CH_3$[a] | O | $CO_2Et$ | 0.013[c] | 2615 |
| **9** | 2,6-di$CH_3$[a] | O | $CO_2Et$ | 0.955 | 78 |
| **10** | 3,5-di$CH_3$[a] | O | $CO_2Et$ | 0.043[c] | ND |
| **10A** | 3,5-di$CH_3$ | O | $CO_2Et$ | 0.236[c] | ND |
| **10B** | 3,5-di$CH_3$ | O | $CO_2Et$ | 0.085[c] | ND |
| **10C** | 3,5-di$CH_3$[b] | O | $CO_2Et$ | 0.036[c] | 1778 |
| **11** | 3,3,5,5-tetra$CH_3$ | O | $CO_2Et$ | 0.258[c] | 112 |
| **12** | 3,5-di$CH_3$[b] | S | $CO_2Et$ | 0.116 | 862 |
| **13** | 3,5-di$CH_3$ [a] | O | H | 0.275 | 200 |
| **14** | H | O | $CO_2H$ | >10[c] | ND |
| **15** | 3,5-di$CH_3$[b] | O | $CH_2OH$ | 0.121 | >826 |
| **16** | 3,5-di$CH_3$[b] | O | $NO_2$ | <0.001 | >37000 |
| **17** | 3,5-di$CH_3$[b] | O | Br | <0.001 | >28000 |
| **18** | 3,5-di$CH_3$[b] | O | $NH_2$ | 1.2[c] | 83 |
| **19** | 3,5-di$CH_3$[b] | O | $NMe_2$ | <0.001 | >66000 |
| **20** | 3,5-di$CH_3$[b] | O | $CH_2N_3$ | <0.001 | >54000 |
| **21** | 3,5-di$CH_3$[b] | O | Me | 0.002 | 40000 |
| **22** | 3,5-di$CH_3$[b] | O | Et | <0.001 | >67000 |
| **23** | 3,5-di$CH_3$[b] | O | *i*-Pr | <0.001 | >82000 |
| **24** | 3,5-di$CH_3$[b] | O | $CMe_2OH$ | <0.001 | >100000 |
| nevirapine | | | | 0.039 | 2564 |
| efavirenz | | | | <0.001 | >58000 |

[a] Mixture of stereoisomers. [b] Stereoisomer with Me substituents in equatorial position. [c] P4 cells.

(∼70%) and **10B** (∼30%). X-ray diffraction allowed the determination of the structure of the major stereoisomer **10A**; it corresponded to the isomer having the oxypyridinone moiety and methyl substituents in the trans position (Figure 4a). A stereoselective Mitsunobu reaction of 3,5-dimethylcyclohexanol ("α isomer"; see Note in the Experimental Section) with **B₀** produced **10C**, a diastereoisomeric form of **10A**, whose structure was confirmed by XRD (Figure 4b). This stereoisomer with all groups in a cis position had a stronger antiviral activity than **10A** (Table 2). This increased potency of **10C** was in agreement with molecular modeling studies. Indeed, docking studies and interaction energy calculations showed that equatorial substitution was more favorable than the axial one (−35.5 kcal/mol for **10C** vs −32.2 kcal/mol for **10A**). The differences between stereoisomers were essentially explained by (i) steric clashes
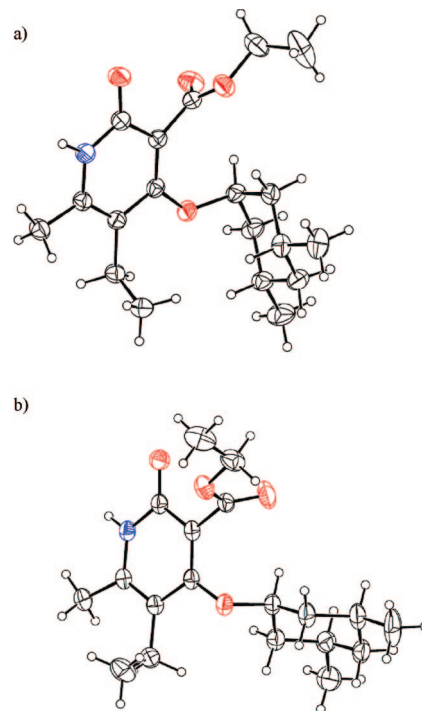


**Figure 4.** X-ray structures of compounds **10A** (a) and **10C** (b) (ORTEP view with displacement ellipsoids drawn at the 50% probability level).[24]

between axial substituents and residues Tyr181/Tyr188 and (ii) favorable van der Waals contacts between equatorial substituents and residue Trp229. Figure 5 shows the optimal fit of **10C** into the allosteric pocket, leading to an excellent inhibitory activity against wild-type HIV-1.

The advantageous equatorial substitution vs axial substitution was also demonstrated by comparing the antiviral activities of **10C** and **11**. Compound **11** with its 3,3,5,5-tetramethyl substituent pattern had a lower antiviral activity than **10C** (Table 2, $EC_{50}$ of 0.258 $\mu$M vs 0.036 $\mu$M). Replacement of 3,5-dimethylcyclohexyloxy by 3,5-dimethylcyclohexylthio moiety in position 4 of the pyridinone ring did not improve the antiviral activity (compound **12** vs **10C**).

While compound **10C** was effective against wild-type HIV-1, it only displayed moderate to poor antiviral activity against Y181C and K103N, two HIV-1 mutant strains often observed in patients treated with NNRTIs (Table 3). Further optimization of **10C** was undertaken in order to replace the hydrolyzable ester group and to obtain inhibitors with a better activity against mutant viral strains.

Structural modifications on position 3 ($R_2$) of the pyridin-2(1*H*)-one ring were performed. Table 2 discloses the activity
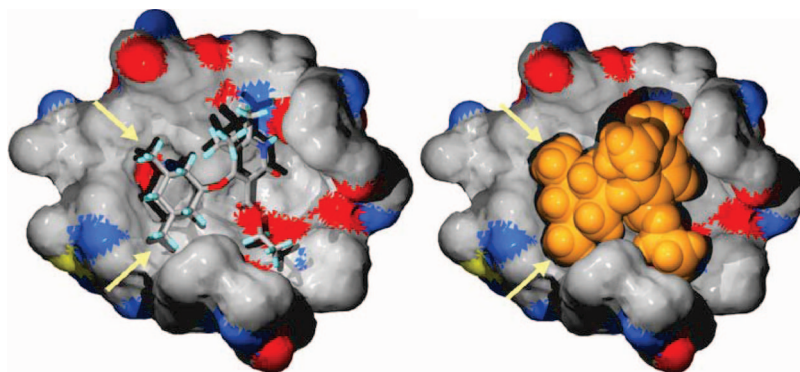
**Figure 5.** View of the optimal fit of **10C** (with methyl groups in equatorial position; yellow arrows) into the allosteric site of RT.

**Table 3.** Antiviral Activity (EC$_{50}$ ($\mu$M)) in TZM-bl Cells, against a Panel of Single-Mutant Strains, of Some Compounds with Substituent Variations at Position 3 of Pyridinone Ring: Comparison with the Reference Compounds Nevirapine and Efavirenz

| compd | Y181C | K103N | L100I | V108I | Y188L |
|---|---|---|---|---|---|
| **10C** | 2.0$^a$ | >10 | 2.2 | 5.9 | >10 |
| **16** | 0.279 | 0.177 | 0.009 | 0.002 | >10 |
| **17** | 0.138 | 0.009 | ND | 0.001 | 6.3 |
| **19** | 0.177 | 0.014 | 0.028 | 0.006 | >10 |
| **20** | 0.206 | 0.074 | 0.034 | 0.011 | >10 |
| **21** | 0.893 | 0.142 | 0.203 | 0.121 | >10 |
| **22** | 0.015 | 0.005 | 0.006 | <0.001 | 5.4 |
| **23** | 0.006 | 0.002 | 0.002 | <0.001 | 1.1 |
| nevirapine | >10 | 3.3 | 0.252 | 0.792 | >10 |
| efavirenz | <0.001 | 0.031 | 0.017 | <0.001 | 0.235 |

$^a$ P4 cells.

of the resulting compounds against wild-type virus in cell culture (P4 or TZM-bl cells). Structure−activity relationships on position 3 (R$_2$) of the pyridine-2(1*H*)-one ring suggested a compromise between occupancy of the binding pocket and the overall lipophilic character of this site. As shown in Table 2, compound **13**, which is not substituted in position 3, was less active than **10**, confirming the importance of filling the hydrophobic pocket. Charged groups appeared clearly unfavorable for activity (**14** vs **2**), suggesting replacement of the hydrolyzable ester moiety of the initial derivatives. Polar neutral groups were better tolerated in this position (**15**, **18**), and compounds displaying weakly polar groups (**16**, **20**) possessed low nanomolar activity. Increased lipophilicity and occupancy of the binding site were clearly beneficial for activity, as demonstrated by compounds **19** and **21**−**24** and by the substantial difference of antiviral potency between compounds **15**−**24** and **18**−**19**. Among lipophilic derivatives, ethyl (**22**) or propyl substituents (**23**) were more favorable than a methyl group (**21**).

A selectivity index (cytotoxicity vs antiviral activity) was also measured for the studied compounds. As shown in Table 2, several derivatives displayed very low toxicity (CC$_{50}$ > 50 $\mu$M) while showing antiviral activity in the subnanomolar range, leading to selectivity indexes over 50 000, which were significantly higher than for nevirapine (2564) and comparable to that for efavirenz (58 000).

Mutant HIV-1 strains were generated by introducing RT mutations that are commonly observed in clinical practice into a wild-type HIV-1 strain.[16] The antiviral activity in a single-round replication assay (TZM-bl cells) against single mutant strains of compounds substituted on position 3 of the pyridin-2(1*H*)-one ring is disclosed in Table 3 and compared with that observed for nevirapine and efavirenz. Mutant strains with single

amino acid substitutions at residues 100, 103, 108, 181 showed only minimally reduced sensitivities to **22** or **23**.

It is now established that a key factor in overcoming viral resistance mutations is the ability of a compound to adapt to the structural changes caused in the binding site by these mutations. While compound flexibility is of prime importance for some mutations,[17] it has also been suggested that the K103N mutation causes resistance by stabilizing the unliganded form of RT.[18] In order to retain activity, RT inhibitors should be able to form additional interactions with the mutated side chain, thereby compensating this stabilization of the unliganded enzyme. In this context, it is especially interesting to note that some pyridinone derivatives might adopt an alternative binding mode when facing mutated binding sites, as suggested by molecular docking results. These binding modes were associated with comparable interaction energies and are illustrated in Figure 6 for compound **22**. The first binding mode (Figure 6a), has been discussed above and pointed the ethyl group in position 3 of the pyridin-2(1*H*)-one ring toward the Pro236 hydrophobic pocket. The second binding mode (Figure 6b) was only favorable in the case of compounds displaying a small and lipophilic group on position 3 and pointed this group toward Tyr181. The preference for small and lipophilic groups in this region has been documented for several series of RT inhibitors, including HEPT derivatives such as TNK-651.[11,19] In the case of the K103N mutation, this alternative binding mode allowed positioning of the carbonyl of the pyridinone ring in the vicinity of the Asn amide group as shown in Figure 6c, suggesting favorable electrostatic interactions between the pyridinone and the mutated side chain. This ability to adopt different binding modes, depending on the structure of the binding site, might explain the ability of compounds **17**, **19**, **22**, and **23** to retain activity against K103N and, possibly, other mutant viral strains (as observed in Table 3).

The activity of the current compounds against the Y188L strain was only in the micromolar range. From Figure 6a, it can be seen that Tyr188 faced the 3,5-dimethylcyclohexyl moiety of the inhibitor and that the position of this group was not modified in the alternative binding mode (Figure 6b). The alternative binding mode was therefore unable to compensate the loss of lipophilic interactions resulting from the Y188L mutation.

We subsequently evaluated several derivatives for their antiviral activity against four clinically relevant double mutant strains using TZM-bl cell assay allowing single-round infection experiment (Table 4). The conclusions from these assays were essentially in line with the results obtained using the single mutant strains. Compounds **22** and **23** displayed the best profile
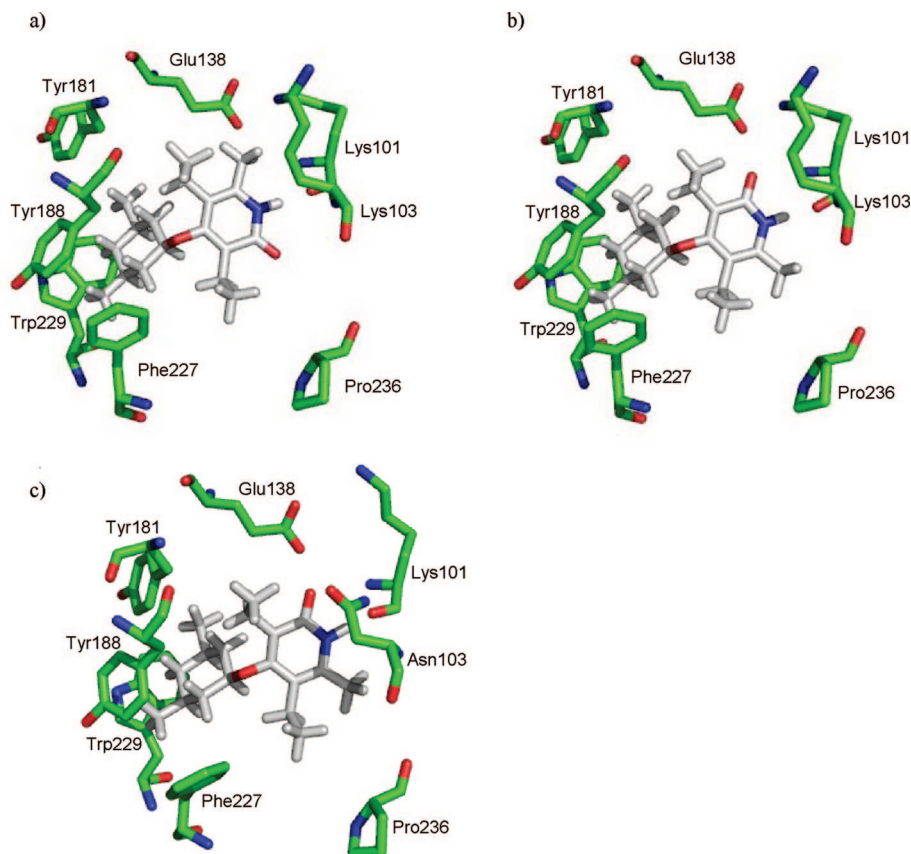
**Figure 6.** Binding modes of **22** into wild-type RT (a and b) and K103N mutant (c).

**Table 4.** Antiviral Activity (EC$_{50}$ ($\mu$M)) in TZM-bl Cells, against a Panel of Double Mutant Strains, of Some Compounds with Substituent Variations at Position 3 of Pyridinone Ring: Comparison with the Reference Compounds Nevirapine and Efavirenz

| compd | K103N/V108I | K103N/Y181C | K103N/L100I | L100I/V108I |
|---|---|---|---|---|
| **16** | ND | >10 | >10 | 8.3 |
| **17** | 0.523 | 0.780 | 0.068 | 0.038 |
| **19** | 0.245 | >10 | 2.9 | 1.6 |
| **20** | 0.689 | 4.4 | 0.828 | 0.107 |
| **21** | 1.2 | 5.1 | 1.4 | 0.833 |
| **22** | 0.359 | 0.107 | 0.081 | 0.115 |
| **23** | 0.642 | 0.105 | 0.044 | 0.010 |
| nevirapine | 6.2 | ≫10 | >10 | >10 |
| efavirenz | 0.525 | 0.034 | 3.7 | 0.014 |

**Table 5.** Antiviral Activity (EC$_{50}$ ($\mu$M)) of Compounds **22** and **23**, against Wild-Type HIV-1 and a Panel of Relevant Mutant Strains, in a Multiple-Round Replication Assay (MT-4 cells): Comparison with the Reference Compound Efavirenz

| compd | WT | Y181C | K103N | L100I | K103N/L100I |
|---|---|---|---|---|---|
| **22** | 0.002 | 0.049 | 0.026 | 0.027 | 0.145 |
| **23** | 0.002 | 0.019 | 0.007 | 0.006 | 0.084 |
| efavirenz | 0.003 | 0.004 | 0.320 | 0.167 | >10 |

against double mutant strains and had an effect comparable or superior to that of efavirenz.

Because of the attractive profile of compounds **22** and **23**, we next decided to test these compounds in parallel with efavirenz in a multiple-round replication assay (MT-4 cells) for their antiviral activity against wild-type HIV-1 as well as several single or double mutant viral strains (Y181C, K103N, L100I, and K103N + L100I). As shown in Table 5, the biological results observed very nicely confirmed those we obtained in the TZM-bl cell assays.

Cell culture selection of mutant virus with greatly reduced susceptibility to the inhibitor **22** resulted in a variant that expressed a combination of substitution (Val106Ala and Phe227Phe/Leu). Both residues are located in the NNRTI binding site (Figure 3). It was previously reported that a high dose of other NNRTIs (S-1153 and UC781) also selected for the V106A plus F227L double mutant.[20,21] The mutations V106A and F227L conferred little resistance to efavirenz as single-point mutations but enhanced the resistance level of viruses carrying these mutations in combination with K103N or Y188L.

## Conclusion

In summary, we have identified a new series of 4-cycloalkyloxypyridin-2(1H)-one derivatives as NNRTIs. The best compounds, **22** and **23**, displayed high potency against wild-type HIV-1 and a panel of single and double mutant strains often observed in patients treated with NNRTIs. Further investigation is ongoing in order to characterize the pharmacokinetic profile of these compounds and to obtain the crystallographic structure of such compounds in complex with RT and mutants.

## Experimental Section

**Chemistry.** ^{1}H NMR spectra were recorded on a Jeol JNM EX-400 spectrometer. Chemical shifts ($\delta$) are reported in parts per million (ppm) downfield from tetramethylsilane (TMS) used as an internal standard. Melting points were determined with a Totolli-Buchi melting point B-545 apparatus. Analytical thin-layer chromatography (TLC) was done on Merck silica gel 60 F$_{254}$ plates. Mass spectra were taken on an ion trap mass spectrometer (ITMS). Elemental analyses (C, H, N, S) were performed on a ThermoFinnigan Flash EA 1112 elemental analyzer at the Pharmacy Department, FUNDP, Namur. HPLC analyses were realized on a Varian 940-LC apparatus with a Varian 380-LC detector.

**Note.** Commercial 3,5-dimethylcyclohexanol (Fluka, purum, 97%) is a mixture of stereoisomers from which the "α isomer" (i.e., equatorial methyl groups and axial OH group) can be separated (∼10%) by column chromatography (eluent ether/pentane, 1:9 v/v). The remaining mixture is subjected to a Mitsunobu reaction (DIAD, PPh₃) with acetic acid, leading to a mixture of acetates in which the "α′ isomer" (i.e., equatorial methyl groups and axial OAc group) is predominating. After basic hydrolysis of the mixture of acetates, chromatographic separation allows recovery of a substantial amount (∼60%) of the desired "α isomer" of 3,5-dimethylcyclohexanol.

**4-(3′,5′-Dimethylcyclohexyloxy)-5-ethyl-3-isopropyl-6-methyl-1*H*-pyridin-2-one (23).** Amounts of 2.25 g (10 mM) of $B_0$, 1.45 g (5.25 mM) of silver carbonate, and 1.25 mL (10.5 mM) of benzyl bromide were placed under argon in a 100 mL two-necked round-bottom flask equipped with a condenser, with a magnetic stirring bar, and with a rubber septum. Then an amount of 30 mL of dry benzene was introduced, and the mixture was heated to 60 °C with stirring for 20 h. After cooling to room temperature, the mixture was diluted with 30 mL of pentane, filtered through a filter agent pad (Celite 521, Aldrich), and evaporated to dryness. The residue was purified by column chromatography (silicagel, eluent pentane/dichloromethane, 1/1 v/v) to give 2.64 g of $B_1$ as a white solid (83% yield).

An amount of 3.22 g (10.2 mM) of $B_1$ was dissolved in 35 mL of dry THF placed under argon in a 200 mL two-necked round-bottom flask fitted with rubber septa. After cooling to −78 °C, a total of 21 mL (33.6 mM) of methyllithium (1.6 M in ether) was added dropwise by means of a syringe. The reaction mixture was kept at −78 °C for 1 h and at 0 °C for 3 h. Then the mixture was diluted with 40 mL of cold ether and slowly neutralized with cold 1 N HCl. The organic layer was separated, and the aqueous phase was extracted twice with 40 mL of ether. The combined organic solution was washed with a saturated sodium bicarbonate solution followed by washing with a saturated sodium chloride solution. After evaporation of the solvents, the residue was purified by column chromatography (silica gel, eluent ether/pentane, 10/90 v/v) to give 2.98 g (97% yield) of alcohol $B_2$.

An amount of 2.39 g (7.94 mM) of $B_2$ was dissolved under argon in 25 mL of dry benzene in a 100 mL two-necked round-bottom flask fitted with a rubber septum. The solution was cooled to 5 °C, and 0.8 mL of thionyl chloride (SOCl₂, 10.9 mM) was added dropwise. After 0.5 h of reaction at 5 °C and 2 h at room temperature, the benzene was evaporated and the residue was dissolved in 40 mL of dichloromethane. This solution was basified with a cold sodium bicarbonate solution, washed with a saturated sodium chloride solution, and dried over magnesium sulfate. Evaporation of the solvent and purification by column chromatography (silica gel, eluent ether/pentane, 5/95 v/v) led to 1.85 g of $B_3$ (82% yield).

Amounts of 294 mg (1.0 mM) of $B_3$, 524 mg (2.0 mM) of triphenylphosphine, and 256 mg (2.0 mM) of 3,5-dimethylcyclo-hexanol ("α isomer") were dissolved under argon in 6 mL of dry THF in a 25 mL two-necked round-bottom flask fitted with a rubber septum and cooled to 0 °C. A total of 406 mg of DIAD (diisopropyl azodicarboxylate, 2.0 mM) dissolved in 2 mL of THF was added dropwise by means of a syringe. The reaction mixture was stirred for 1 h at 0 °C, then for 20 h at room temperature. After evaporation of the volatiles, the residue was triturated in 20 mL of pentane for 0.5 h and filtered and the pentane solution was washed with 5 mL of sodium hydroxide (0.5 N), with water and with saturated sodium chloride. After drying over magnesium sulfate and evaporation of the solvent, the product was purified by column chromatography (silica gel, eluent ether/pentane, 2.5/97.5 v/v) to give 340 mg (84% yield) of $B_4$.

An amount of 6 g (15.3 mM) of $B_4$ was dissolved in 100 mL of absolute ethanol in a 250 mL two-necked round-bottom flask fitted with rubber septa. Then 1 g of palladium on carbon (10 wt %) was introduced, and the mixture was placed under hydrogen (1 atm) and stirred at room temperature for 36 h. After filtration through a filter agent pad (Celite 521, Aldrich), the solvent was evaporated and the solid residue was crystallized from absolute ethanol to give

4.53 g (97% yield) of **23**. ¹H NMR (CDCl₃, 400 MHz): δ 1.0 (d, 6H, CH₃³′ and CH₃⁵′), 1.1 (m, 3H, 5-CH₂CH₃), 1.4 (d, 6H, 3-CH(CH₃)₂), 0.6−2.0 (m, 8H, cyclohexyl), 2.3 (s, 3H, 6-CH₃), 2.45 (q, 2H, 5-CH₂CH₃), 3.2 (m, 1H, 3-CH(CH₃)₂), 3.85 (m, 1H, H¹′), 12.4 (s, 1H, NH). Mp 184 °C. MS: (M + H)⁺ 306.0. Anal. (C₁₉H₃₁NO₂) C: calcd, 74.71; found, 75.67. H: calcd, 10.23; found, 10.24. N: calcd, 4.59; found, 4.31. Purity by HPLC, 99%.

**4-(3′,5′-Dimethylcyclohexyloxy)-3,5-diethyl-6-methyl-1*H*-py-ridin-2-one (22).** A solution of diethyl 2-ethylmalonate (13.16 g, 0.07 M) in 15 mL of toluene was added to 20 mL of a 3.75 M solution of EtONa in EtOH freshly prepared, and the mixture was heated to 80 °C for 30 min. Then a solution of ethyl 2-ethyl-3-aminocrotonate (11 g, 0.07 M) in 20 mL of toluene was added, and the mixture was refluxed for 60 h. After the mixture was cooled, an amount of 150 mL of water was added under thorough mixing, leading to a two phase system. The water layer was separated (it contained the sodium salt of **A**), washed twice with 20 mL of toluene, and neutralized with concentrated hydrochloric acid to pH 7. The precipitate was filtered, washed with water, and dried to give 8 g (60% yield) of intermediate **A**.

Amounts of 3.62 g (0.02 M) of intermediate **A**, 5.5 g (0.02 M) of silver carbonate, and 3.42 g (0.02 M) of benzyl bromide were placed in 50 mL of benzene and heated to 80 °C for 6 h. After cooling to room temperature, the mixture was filtered and the solvent was evaporated. The crude product was purified by column chromatography (silica gel, eluent pentane/dichloromethane, 50/50 v/v %) to give 4.33 g (80% yield) of intermediate **B**.

To a solution of 2.71 g (0.01 M) of compound **B**, 2.56 g (0.02 M) of 3,5-dimethylcyclohexanol ("α isomer"), and 5.26 g (0.02 M) of triphenylphosphine in 50 mL of THF, 4 g (0.02 M) of diisopropyl azodicarboxylate (DIAD) was added dropwise at room temperature, and the mixture was stirred overnight. The solvent THF was evaporated, and the pasty residue was triturated in 100 mL of hexane. The undissolved solid (triphenylphosphine oxide) was filtered off, and the solvents were evaporated. The crude product was purified by column chromatography (silica gel, eluent pentane/dichloromethane, 50/50 v/v %) to give 2.65 g (70% yield) of intermediate **C**.

Amounts of 0.381 g (0.001 M) of intermediate **C**, 4 mL of cyclohexene, and 0.2 g of Pd/C 10% were placed in 12 mL of diisopropyl ether, and the mixture was heated to 80 °C for 6 h. The mixture was filtered, and the volatiles were evaporated. The residue was purified by column chromatography (silica gel, eluent ethanol/dichloromethane, 5/95 v/v %) to give 0.262 g (90% yield) of compound **22**. ¹H NMR (CDCl₃, 400 MHz): δ 0.9 (d, 6H, CH₃³′ and CH₃⁵′), 1.05 (m, 3H, 5-CH₂CH₃), 1.15 (m, 3H, 3-CH₂CH₃), 0.6−2.1 (m, 8H, cyclohexyl), 2.35 (s, 3H, 6-CH₃), 2.5 (q, 2H, 5-CH₂CH₃), 2.6 (q, 2H, 3-CH₂CH₃), 3.9 (m, 1H, H¹′), 12.8 (s, 1H, NH). Mp 160−161 °C. MS: (M + H)⁺ 292.41. Anal. (C₁₈H₂₉NO₂) C: calcd, 74.18; found, 73.94. H: calcd, 10.03; found, 9.86. N: calcd, 4.81; found, 4.58. Purity by HPLC, 99.0%.

**Molecular Modeling. Docking Studies.** Docking of the inhibitors into RT was carried out using GOLD (version 1.1) programs.[12] GOLD uses a genetic algorithm and performs flexible ligand docking into proteins with partial flexibility in the neighborhood of the active site. Some limited flexibility of the binding site is taken into account by optimizing the torsion angles of Ser, Thr, and Tyr hydroxyl groups as well as Lys NH₃⁺ moieties during the docking run so that hydrogen bond formation is favored. Default settings were used for the genetic algorithm parameters.

Display and examination of the docking poses were carried out using the Insight II environment.[14]

**Energy Minimization.** In order to better take into account protein flexibility, docking poses were refined with Discover 3 (CVFF force field, dielectric constant 1*r).[13] Our energy minimization process included two sequential steps: a "steepest descent" algorithm, reaching a convergence of 10.0 kcal mol⁻¹ Å⁻¹, followed by a "conjugate gradient" minimization to reach a final convergence of 0.01 kcal mol⁻¹ Å⁻¹. All protein atoms were first kept fixed, while the orientation of the inhibitor was optimized. Receptor side chains within 12 Å of the inhibitor were then progressively relaxed,

using degressive restraints (quadratic form, initial force constant of 20.0 kcal mol$^{-1}$ Å$^{-2}$).

**X-ray Diffraction.** Crystals were obtained by slow evaporation of a cyclohexane solution for **10A** and an isooctane solution for **10C** at room temperature. X-ray intensities were collected on a graphite-monochromated CAD-4 Enraf-Nonius diffractometer with Cu K$_\alpha$ radiation ($\lambda$ = 1.54178 Å) using $\theta$−$2\theta$ scan technique. Lorentz, polarization, and analytical absorption corrections were applied. The structure was solved using PLATON (combining SIR97 software for solving and SHELXL97 for refinement).[24] Non-hydrogen atoms were refined anisotropically, while hydrogen atoms were calculated geometrically (except NH hydrogen refined on position and with isotropic displacement parameters).

**Biological Assays. Cells and Viruses.** The following reagents were obtained through the AIDS Research and Reference Reagent Program, Division of AIDS, NIAID, NIH. The TZM-bl cell line was from Dr. John C. Kappes, Dr. Xiaoyun Wu, and Tranzyme Inc., and the MT-4 cell line was from Dr. Douglas Richman.

The TZM-bl cells were cultured in DMEM medium (Invitrogen) supplemented with 5% (v/v) heat-inactivated fetal bovine serum, 50 U of penicillin/mL, and 50 $\mu$g of streptomycin/mL (Invitrogen). Exponentially growing cells were trypsinized, centrifuged, and split twice weekly. The HTLV-I transformed T4 cell line (MT-4) was cultured in RPMI 1640 medium (Invitrogen) supplemented with 10% (v/v) heat-inactived fetal bovine serum, 50 U of penicillin/mL, and 50 $\mu$g of streptomycin/mL (Invitrogen). All cells were grown at 37 °C in a 5% CO$_2$ atmosphere. The HIV strain used in this study is HIV-1 NL4-3 derived from the infectious molecular clone pNL4-3. HIV-1 stocks were stored as cell-free supernatants at −80 °C.

**Reverse Transcriptase Assays.** Enzyme activities were determined by following the incorporation of [$^{32}$P]dGTP into a homopolymeric template/primer substrate, poly(rC)-oligo(dG)$_{12-18}$. The RT assays using recombinant HIV-1 RT (Calbiochem) were performed in a final volume of 50 $\mu$L. Briefly, the reaction mixture contained 50 mM Tris-HCl, pH 8.3, 50 mM KCl, 10 mM MgCl$_2$, 2 mM DTT, 10 $\mu$g of BSA, 0.01% Triton X100, 20 $\mu$g/mL poly(rC)-oligo(dG)$_{12-18}$ (Amersham), a fixed concentration of the labeled substrate (1 $\mu$Ci per assay [$^{32}$P]dGTP), a fixed concentration of the inhibitor (10 $\mu$M, dissolved in 1 $\mu$L of dimethyl sulfoxide). After a 10 min of incubation at 37 °C, the reaction mixtures were chilled on ice and collected on a DEAE-Filtermat (Perkin-Elmer). After washing with 5% Na$_2$HPO$_4$ and H$_2$O, the amount of radioactivity was determined by phosphorimager counting. The in vitro activity of the compounds, at a final concentration of 10 $\mu$M, on the HIV-1 RT activity was derived from the relative reduction in RT activity. The RT activity in the absence of any compound was arbitrarily assigned a value of 100% of activity.

**Anti-HIV in Cultured Cell Lines.** Antiviral activity of the compounds was tested either in the P4 cell line[22] or in the TZM-bl cell line.[23] Both cell lines use a Tat protein-induced transactivation of the $\beta$-galactosidase gene driven by the HIV-1 LTR promoter. In brief, exponentially growing cells were plated at 5000 cells/well in flat-bottom 96-well microtiter plates. After 48 h of incubation, the medium was removed and replaced by 100 $\mu$L of medium containing the pyridinone derivatives at concentrations ranging from 0.00128 to 4 $\mu$M. Four hours after drug addition, cells were infected with an equal amount of cell-free virus (NL4-3 strain) corresponding to 100 ng of HIV p24 antigen. At 48 h postinfection, the medium was removed and cells were lysed in PBS containing 0.1% NP-40 and 5 mM MgCl$_2$. $\beta$-Galactosidase activity was measured using chlorophenol red $\beta$-D-galactopyranoside (Roche) assays. The 50% effective concentration (EC$_{50}$) was calculated from each dose−response curve using the CurveExpert1.3 software.[25]

**Cytotoxicity of the Compounds.** Flat-bottom 96-well plates were filled with 50 $\mu$L of complete medium containing 5000 TZM-bl or P4 cells. Two hours later, 50 $\mu$L of medium containing an appropriate dilution of the test compounds (from 100 to 0.032 $\mu$M) was added. Cells and compounds were incubated at 37 °C in growth medium for 3 days. Cell viability was determined by a colorimetric

assay based on the cleavage of the tetrazolium salt WST-1 (Roche) by mitochondrial dehydrogenases in viable cells. Absorbance of converted dye was measured in an ELISA plate reader at a wavelength of 570 nm. The cytotoxicity of the compounds was calculated as the reduction (in %) of viable cells compared with the drug-free control culture. The drug concentration required to reduce cell viability by 50% was named CC$_{50}$.

**Activity of Compounds in the MT-4 Assay.** The most active compounds **22** and **23** were tested in a multiple-round replication assay using the MT-4 human T-cell line. MT-4 cells were infected with wild-type HIV-1 (NL4-3 strain) or mutant HIV-1 strains and then exposed to different concentrations of antiviral compounds. After 5 days of incubation, the viability of HIV-infected and mock-infected cells was determined by a colorimetric assay based on the cleavage of the tetrazolium salt WST-1 (Roche). This method, based on the protocol originally described by Pauwels et al.,[26] allows simultaneous determination of the 50% inhibitory concentration (EC$_{50}$) for inhibiting viral cytopathicity and the 50% cytotoxic concentration (CC$_{50}$).

**Production of Viral Mutants.** In vitro mutagenesis was applied to the RT-coding region of the infectious molecular clone pNL4-3 to obtain drug-resistant mutant strains. The following mutations were separately introduced in pNL4-3: L100I, K103N, V108I, Y181C, Y188L, and the double mutations K103N/L100I, K103N/V108I, K103N/Y181C, L100I/V108I. These mutations were chosen because of the resistance they confer to existing NNRTIs. Plasmids were checked by sequencing to confirm that they contained the desired mutations. The mutant clones were transfected in HEK293 cells. The virus stocks were prepared from the cell-free supernatant at day 2 or 3 posttransfection.

**In Vitro Selection of HIV-1 Mutant Strains.** CEM cells were infected with a highly infectious HIV-1 clone, HIV-1 IIIB, at high MOI and were exposed to **22** or **23** initially at 5-fold the 50% effective concentration (EC$_{50}$). Infected cells were incubated for 4 days. The RT activities in the culture supernatants were assayed, and then the cells were diluted 1:4 in fresh medium containing the antiviral agents. The dose of **22** was modified according to the CPE observed in the cells. If the virus was replicating (as evidenced by a visible CPE or a high dose of RT activity), the dose of the agent was increased 5-fold in the following 1:4 dilution. Cells were diluted as described above twice a week.[27]

**Determination of the Amino Acid Sequence of the RT of Drug-Resistant Virus Strains.** CEM cells infected with the HIV-1 mutant strains were subjected to total DNA isolation. The RT regions in the resistant variants were PCR-amplified, purified, and sequenced as previously described.[27]

**Supporting Information Available:** Experimental and spectroscopic data for compounds **1**−**21** and **24** and HPLC data verifying the purities of compounds **1**−**24**. This material is available free of charge via the Internet at http://pubs.acs.org.

## References

(1) De Clercq, E. New developments in anti-HIV chemotherapy. *Curr. Med. Chem.* **2001**, *8* (13), 1543–1572.

(2) Smerdon, S. J.; Jäger, J.; Wang, J.; Kohlstaedt, L. A.; Chirino, A. J.; Friedman, J. M.; Rice, P. A.; Steitz, T. A. Structure of the binding site for non nucleoside inhibitors of the reverse transcriptase of human immunodeficiency virus type 1. *Proc. Natl. Acad. Sci. U.S.A.* **1994**, *91*, 3911–3915.

(3) Arnold, E.; Das, K.; Ding, J.; Yadav, P. N. S.; Hsiou, Y.; Boyer, P. L.; Hughes, S. H. Targeting HIV reverse transcriptase for anti-AIDS drug design: structural and biological considerations for chemotherapeutic strategies. *Drug Des. Discovery* **1996**, *13*, 29–47.

(4) (a) De Clercq, E. Non nucleoside reverse transcriptase inhibitors (NNRTI): past, present and future. *Chem. Biodiversity* **2004**, *1*, 44–64. (b) Minuto, J. J.; Haubrich, R. Etravirine: a second-generation NNRTI for treatment-experienced adults with resistant HIV-1 infection. *Future HIV Ther.* **2008**, *2* (6), 525–537.

(5) (a) Hammer, S. M.; Saag, M. S.; Schechter, M.; Montaner, J. S.; Schooley, R. T.; Jacobsen, D. M.; Thompson, M. A.; Carpenter, C. C.; Fischl, M. A.; Gazzard, B. G.; Gatell, J. M.; Hirsch, M. S.; Katzenstein, D. A.; Richman, D. D.; Vella, S.; Yeni, P. G.; Volberding, P. A. Treatment for adult HIV infection: 2006 recommendations of the International AIDS Society–USA panel. *JAMA, J. Am. Med. Assoc.* **2006**, *296* (7), 827–843. (b) De Clercq, E. Anti-HIV drugs: 25 compounds approved within 25 years after the discovery of HIV. *Int. J. Antimicrob. Agents* **2009**, *33* (4), 307–320.

(6) Hirsch, M. S.; Brun-Vezinet, F.; Clotet, B.; Conway, B.; Kuritzkes, D. R.; D'Aquila, R. T.; Demeter, L. M.; Hammer, S. M.; Johnson, V. A.; Loveday, C.; Mellors, J. W.; Jacobson, D. M.; Richman, D. D. Antiretroviral drug resistance testing in adults infected with human immunodeficiency virus type 1: 2003 recommendations of an International AIDS Society–USA Panel. *Clin. Infect. Dis.* **2003**, *37*, 113–128.

(7) Goldman, M. E.; Nunberg, J. H.; O'Brien, J. A.; Quintero, J. C.; Schleif, W. A.; Freund, K. F.; Gaul, S. L.; Saari, W. S.; Wai, J. S. Pyridinone derivatives: specific human immunodeficiency virus type 1 reverse transcriptase inhibitors with antiviral activity. *Proc. Natl. Acad. Sci. U.S.A.* **1991**, *88* (15), 6863–6867.

(8) Dolle, V.; Fan, E.; Nguyen, C. H.; Aubertin, A.-M.; Kirn, A.; Andreola, M. L.; Jamieson, G.; Tarrago-Litvak, L.; Bisagni, E. A new series of pyridinone derivatives as potent non-nucleoside human immunodeficiency virus type 1 specific reverse transcriptase inhibitors. *J. Med. Chem.* **1995**, *38* (23), 4679–4686.

(9) Dolle, V.; Nguyen, C. H.; Legraverend, M.; Aubertin, A.-M.; Kirn, A.; Andreola, M. L.; Ventura, M.; Tarrago-Litvak, L.; Bisagni, E. Synthesis and antiviral activity of 4-benzyl pyridinone derivatives as potent and selective non-nucleoside human immunodeficiency virus type 1 reverse transcriptase inhibitors. *J. Med. Chem.* **2000**, *43* (21), 3949–3962.

(10) Benjahad, A.; Croisy, M.; Monneret, C.; Bisagni, E.; Mabire, D.; Coupa, S.; Poncelet, A.; Csoka, I.; Guillemont, J.; Meyer, C.; Andries, K.; De Bethune, M.-P.; Himmel, D. M.; Das, K.; Arnold, E.; Nguyen, C. H.; Grierson, D. S. 4-Benzyl and 4-benzoyl-3-dimethylaminopyridin-2(1*H*)-ones: in vitro evaluation of new C-3-amino-substituted and C-5,6-alkyl-substituted analogues against clinically important HIV mutant strains. *J. Med. Chem.* **2005**, *48* (6), 1948–1964.

(11) Hopkins, A. L.; Ren, J.; Esnouf, R. M.; Willcox, B. E.; Jones, E. Y.; Ross, C.; Miyasaka, T.; Walker, R. T.; Tanaka, H. Complexes of HIV-1 reverse transcriptase with inhibitors of the HEPT series reveal conformational changes relevant to the design of potent non-nucleoside Inhibitors. *J. Med. Chem.* **1996**, *39* (8), 1589–1600.

(12) Jones, G.; Willett, P.; Glen, R. C.; Leach, A. R.; Taylor, R. Development and validation of a genetic algorithm for flexible docking. *J. Mol. Biol.* **1997**, *267* (3), 727–748.

(13) *Discover 3*; Accelrys Inc.: San Diego, CA.

(14) *Insight II*; Accelrys Inc.: San Diego, CA.

(15) Himmel, D. M.; Das, K.; Clark, A. D., Jr.; Hughes, S. H.; Benjahad, A.; Oumouch, S.; Guillemont, J.; Coupa, S.; Poncelet, A.; Csoka, I.; Meyer, C.; Andries, K.; Nguyen, C. H.; Grierson, D. S.; Arnold, E. Crystal structures for HIV-1 reverse transcriptase in complexes with three pyridinone derivatives: a new class of non-nucleoside inhibitors effective against a broad range of drug-resistant strains. *J. Med. Chem.* **2005**, *48* (24), 7582–7591.

(16) Bacheler, L.; Jeffrey, S.; Hanna, G.; D'Aquila, R.; Wallace, L.; Logue, K.; Cordova, B.; Hertogs, K.; Larder, B.; Buckery, R.; Baker, D.; Gallagher, K.; Scarnati, H.; Tritch, R.; Rizzo, C. Genotypic correlates of phenotypic resistance to efavirenz in virus isolates from patients failing nonnucleoside reverse transcriptase inhibitor therapy. *J. Virol.* **2001**, *75* (11), 4999–5008.

(17) (a) Das, K.; Lewi, P. J.; Hugues, S. H.; Arnold, E. Crystallography and the design of anti-AIDS drugs: conformational flexibility and positional adaptability are important in the design of non-nucleoside HIV-1 reverse transcriptase inhibitors. *Prog. Biophys. Mol. Biol.* **2005**, *88*, 209–231. (b) Ren, J.; Stammers, D. K. Structural basis for drug resistance mechanisms for non-nucleoside inhibitors of HIV reverse transcriptase. *Virus Res.* **2008**, *134* (1−2), 157–170.

(18) Hsiou, Y.; Ding, J.; Das, K.; Clark, A. D., Jr.; Boyer, P. L.; Lewi, P.; Janssen, P. A.; Kleim, J.-P.; Rösner, M.; Hughes, S. H.; Arnold, E. The Lys103Asn mutation of HIV-1 RT: a novel mechanism of drug resistance. *J. Mol. Biol.* **2001**, *309*, 437–445.

(19) Tanaka, H.; Baba, M.; Hayakawa, H.; Sakamaki, T.; Miyasaka, T.; Ubasawa, M.; Takashima, H.; Sekiya, K.; Nitta, I.; Shigeta, S.; Walker, R. T.; Balzarini, J.; De Clercq, E. A new class of HIV-1 specific 6-substituted acyclouridine derivatives: synthesis and anti-HIV-1 activity of 5- or 6-substituted analogs of 1-[(2-hydroxyethoxy)methyl]-6-(phenylthio)thymine (HEPT). *J. Med. Chem.* **1991**, *34* (1), 349–357.

(20) Fujiwara, T.; Sato, A.; el-Farrash, M.; Miki, S.; Abe, K.; Isaka, Y.; Kodama, M.; Wu, Y.; Chen, L. B.; Harada, H.; Sugimoto, H.; Hatanaka, M.; Hinuma, Y. S-1153 inhibits replication of known drug-resistant strains of human immunodeficiency virus type 1. *Antimicrob. Agents Chemother.* **1998**, *42* (6), 1340–1345.

(21) Balzarini, J.; Pelemans, H.; Esnouf, R.; De Clercq, E. A novel mutation (F227L) arises in the reverse transcriptase of human immunodeficiency virus type 1 on dose-escalating treatment of HIV type 1-infected cell cultures with the nonnucleoside reverse transcriptase inhibitor thiocarboxanilide UC-781. *AIDS Res. Hum. Retroviruses* **1998**, *14* (3), 255–260.

(22) Clavel, F.; Charneau, P. Fusion from without directed by human immunodeficiency virus particles. *J. Virol.* **1994**, *68* (2), 179–185.

(23) Wei, X.; Decker, J. M.; Liu, H.; Zhang, Z.; Arani, R. B.; Kilby, J. M.; Saag, M. S.; Wu, X.; Shaw, G. M.; Kappes, J. C. Emergence of resistant human immunodeficiency virus type 1 in patients receiving fusion inhibitor (T-20) monotherapy. *Antimicrob. Agents Chemother.* **2002**, *46* (6), 1896–1905.

(24) Spek, A. L. *PLATON*; University of Utrecht: Utrecht, The Netherlands, 2001.

(25) CurveExpert1.3: A Comprehensive Curve Fitting Package for Windows.

(26) Pauwels, R.; Balzarini, J.; Baba, M.; Snoeck, R.; Schols, D.; Herdewijn, P.; Desmyter, J.; De Clercq, E. Rapid and automated tetrazolium-based colorimetric assay for the detection of anti-HIV compounds. *J. Virol. Methods.* **1988**, *20* (4), 309–321.

(27) Stevens, M.; Pannecouque, C.; De Clercq, E.; Balzarini, J. Inhibition of HIV by a new class of pyridine oxide derivatives. *Antimicrob. Agents Chemother.* **2003**, *47* (9), 2951–2957.